Oxidation of Imidazolepentacyanoiron(II) by Hydrogen Peroxide

Mark L. Bowers, Dan Kovacs, and Rex E. Shepherd*

Contribution from the Department of Chemistry, University of Pittsburgh, Pittsburgh, Pennsylvania 15260. *Received March 17, 1977*

Abstract: The oxidations of $(CN)_5Fe(imz)^{3-}$ and $(CN)_5Fe(N\text{-}CH_3imz)^{3-}$ by H_2O_2 proceed by dissociation of the corresponding imidazole and rate-limited substitution of H_2O_2. Hydroxyl radical formed in the initial one-electron reduction of H_2O_2 is scavenged competitively by $(CN)_5Fe(imz\text{-}R)^{3-}$, H_2O_2, or organic components (RH). H_2EDTA^{2-} is inhibitory; *tert*-butyl alcohol, imidazole, and acrylonitrile are kinetically equivalent to HO· itself. Substitution of the imidazoles on $(CN)_5FeH_2O^{3-}$ was followed by competition with 2-methylpyrazine. Values of the second-order substitution rate constants are 410 ± 30 (imz), 418 ± 20 ($N\text{-}CH_3imz$), 323 ± 6 $M^{-1}\ s^{-1}$ ($2CH_3pz$) at 25.0 °C, $\mu = 0.10$, phosphate buffer. The dissociation of the $(CN)_5Fe(imz\text{-}R)^{3-}$ complexes occurs with $\Delta H^{\ddagger} = 21.5 \pm 0.5$ kcal/mol, $\Delta S^{\ddagger} = +1 \pm 2$ eu, $k_{298} = (2.20 \pm 0.21) \times 10^{-3}\ s^{-1}$ (imz); $\Delta H^{\ddagger} = 19.5 \pm 0.5$ kcal/mol, $\Delta S^{\ddagger} = -5 \pm 2$ eu, $k_{298} = (3.24 \pm 0.22) \times 10^{-3}\ s^{-1}$ ($N\text{-}CH_3imz$). The stoichiometry for the reduction of H_2O_2 by $(CN)_5Fe(imz\text{-}R)^{3-}$ is 0.50 at limiting initial time. The Fe(III) product complexes, or species in equilibrium with them, catalyze the decomposition of H_2O_2 into O_2. The rate of decomposition is dependent on $[H_2O_2]^2$ and $[(CN)_5Fe(imz\text{-}R)^{2-}]$ with $k_d = 8.4 \times 10^{-8}\ M^{-2}\ s^{-1}$, $\mu = 0.10$, $T = 25.0$ °C, in the presence of 0.01 M H_2EDTA^{2-}.

The coordination of histidine as an axial ligand for iron in the cytochromes and heme proteins promotes an interest in the coordination of imidazole with low-spin Fe(II) and Fe(III) complexes.[1-4] We recently characterized N-3 bound imidazole and histidine complexes of $(CN)_5Fe^{3-}$ and $(CN)_5Fe^{2-}$ moieties.[5] This report describes the kinetics of the oxidation of $(CN)_5Fe(imz)^{3-}$ and $(CN)_5Fe(N\text{-}CH_3imz)^{3-}$ by H_2O_2. Initially, we had hoped that a study of this system might provide evidence for imidazyl or Fe(III) imidazyl intermediates similar to those proposed by Wang as radical precursors in the ATP synthesis within mitochondria and related model systems.[6] The data obtained for the oxidation of $(CN)_5Fe(imz)^{3-}$ by H_2O_2 support a dissociative mechanism. Loss of imidazole from $(CN)_5Fe(imz)^{3-}$ and substitution of H_2O_2 into the inner coordination sphere of $(CN)_5FeH_2O^{3-}$ are rate determining. Our results are in harmony with the general observation that reduction of H_2O_2 by metal centers having labile coordination sites is about 10^4 faster than when H_2O_2 is restricted to an outer-sphere role.[7] The thermally accessible dissociation of imidazole from $(CN)_5Fe(imz)^{3-}$ provides catalysis via $(CN)_5FeH_2O^{3-}$ for reaction with H_2O_2. The observed thermal pathway is similar to the path observed in the oxidation of $Fe(CN)_6^{4-}$ by H_2O_2 which is activated by photodissociation of CN^-.[8] The hydroxyl radical which is formed either reacts with a second mole of $(CN)_5Fe(imz)^{3-}$ or it may be intercepted by other organic molecules present in the reaction medium. The resultant organic radicals may be separated into several classes on the basis of their reactivity toward the Fe(II) and Fe(III) species in the system. The differentiation parallels the observations of Walling for the reactivity of organic radicals produced by Fenton's reagent and the H_2O_2/Fe(EDTA)$^{2-}$ system.[9] A substantial catalase activity has been observed for the $(CN)_5Fe(imz)^{2-}$ product.

Experimental Section

$(CN)_5Fe(imz)^{3-}$ and $(CN)_5Fe(N\text{-}CH_3imz)^{3-}$ Solutions. The $(CN)_5FeL^{3-}$ solutions were prepared immediately before use by combining weighed amounts of the desired imidazole, dissolved in Ar or N_2 purged buffer, with weighted samples of $Na_3[(CN)_5FeNH_3]\cdot 3H_2O$.[5] All manipulations of the Fe(II) imidazole complex solutions were carried out using syringe or inert atmosphere techniques. Platinum or Teflon needles were used to eliminate contact with catalytic sources of iron. Samples were protected by subdued light with aluminum foil wrapped vessels.

$(CN)_5Fe(imz)^{2-}$ Solutions. $(CN)_5Fe(imz)^{2-}$ was prepared for kinetic and equilibrium studies by oxidation of $(CN)_5Fe(imz)^{3-}$ with H_2O_2. The $(CN)_5Fe(imz)^{2-}$ product was separated from excess H_2O_2 and ligand by means of anion exchange on AG-4X resin in either the Cl^- or SO_4^{2-} form. The product was isolated immediately from the resin phase by solutions of NaCl at the desired ionic strengths. Samples were stored at 5 °C in the dark with known amounts of free ligand imidazole readded to suppress the conversion of $(CN)_5Fe(imz)^{2-}$ into $Fe_2(CN)_{10}^{4-}$ dimeric ions.[10,11] Catalase activity studies were carried out in black-painted volumetric flasks, additionally wrapped in aluminum foil and suspended in a constant temperature bath at 25.0 °C.

H_2O_2 Analysis. The H_2O_2 was titrated by standard $(NH_4)_2Ce(NO_3)_6$ solution in H_2SO_4. H_2O_2, determined on aliquots for the catalase and stoichiometry experiments, was separated from other components of the reaction medium by passage through AG-4X resin in the SO_4^{2-} form. The aliquot with H_2O was titrated by Ce(IV).

Rapid Scan Spectra. The oxidation of $(CN)_5Fe(imz)^{3-}$ by H_2O_2 was examined from 250 to 550 nm by a Vidicon rapid scanning spectrophotometer.[12] Absorbance data as a function of wavelength and time were stored for recall in a PDP12 computer. Wavelength and intensity calibrations were carried out on each run by storage of the spectrum of holmium oxide glass as a reference.

Stopped-Flow Kinetic Data. Data for the oxidation of $(CN)_5Fe(imz)^{3-}$ were obtained using a Durrum D-110 stopped-flow with appropriate temperature control equipment. The photomultiplier output was converted to absorbance and displayed on a Tektronix storage oscilloscope. The data record was obtained by photographing the scope. Reactions lasting longer than could be easily displayed over 50 s on the oscilloscope were recorded with a Houston 2000 X-Y recorder with a calibrated time base. Results obtained in this manner were in agreement with preliminary data obtained on a computer-interfaced stopped-flow instrument.[12] The final absorbance was checked against the Beer's law calculated (ϵ $1.15 \times 10^3\ M^{-1}\ cm^{-1}$ for $(CN)_5Fe(imz)^{2-}$ at 403 nm) value, based on the weight of $Na_3[Fe(CN)_5NH_3]\cdot 3H_2O$ used to prepare $(CN)_5Fe(imz)^{3-}$.

UV-Visible Spectra. Spectra were obtained on a Varian-Cary 118 spectrophotometer with a thermostated sample compartment. Dissociation kinetics of imidazole and *N*-methylimidazole from $(CN)_5Fe^{3-}$ were followed at 450 nm by scavenging $(CN)_5FeH_2O^{3-}$ with 2-methylpyrazine.[5] Equilibrium studies with $(CN)_5Fe(imz)^{2-}$ and NCS^- were monitored at the 590-nm maximum of $(CN)_5FeSCN^{3-}$ where ϵ 2700 $M^{-1}\ cm^{-1}$.[13,14] Reactants for the dissociation experiments and equilibrium studies were flushed with N_2 and temperature equilibrated prior to mixing. The mixed solution was transferred in a syringe operation to a spectrophotometric cell which was capped with a septum, preflushed with N_2, and equilibrated at the same temperature of the cell compartment.

Buffers and pH Measurements. The pH of the reaction solutions was monitored with an Orion 601 digital pH meter standardized with commercial buffers. Buffer solutions were prepared from analytical weights of known sodium buffer salts.

Kinetic results were reproducible from different sources of buffer salts. Because the decomposition of H_2O_2 is very sensitive to iron and

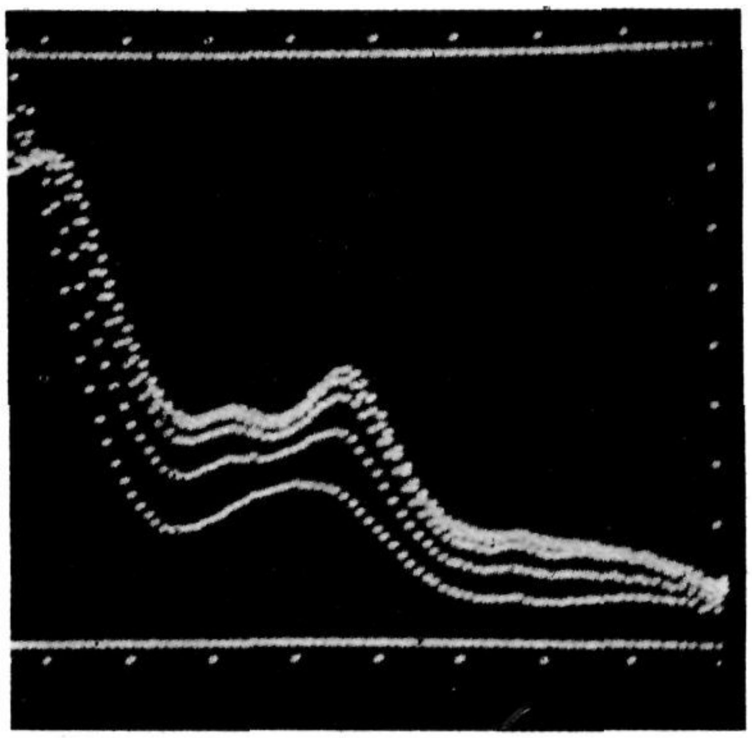

Figure 1. Rapid scan spectra: curves (lowest to highest) at 1.0, 5.0, 20.0, 40.0, and 56.0 s; absorbance 0.00 to 0.50; wavelength 279 to 539 nm; maxima at 294, 357, 403 nm; $[(CN)_5Fe(imz)^{3-}] = 9.70 \times 10^{-4}$ M; $[H_2O_2] = 2.00 \times 10^{-2}$ M; $\mu = 0.10$, $T = 25$ °C.

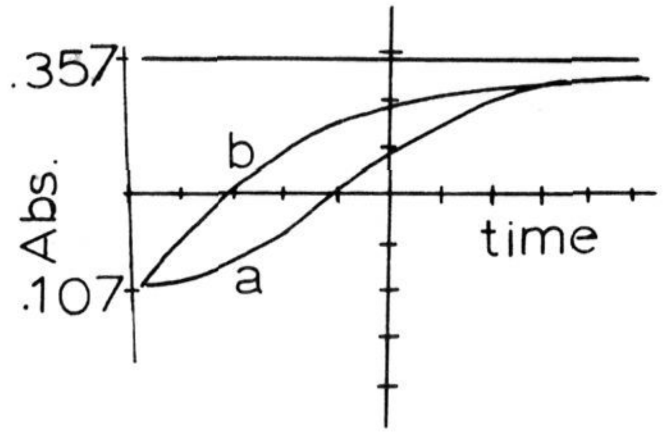

Figure 2. Oscilloscopic data recording of $(CN)_5Fe\ imz^{3-}/H_2O_2$ reaction at 403 nm: (a) $[(CN)_5Fe(imz)^{3-}] = 2.55 \times 10^{-4}$ M, $[H_2O_2] = 0.103$ M, pH 7.00 phosphate buffer, $\mu = 0.1$, time base = 2.00 s/div, $[imz] = [Fe(II)]_{tot}$; (b) same conditions as (a) except that $[imz] = 9.90 \times 10^{-3}$ M + $[Fe(II)]_{tot}$ and time base = 5.00 s/div.

copper impurities in salts, the reproducibility implies that the salts contained an acceptable minimum of contamination. A few early experiments illustrated that presence of metallic impurities will dramatically and erratically alter the observed rate of reaction between $(CN)_5Fe(imz)^{3-}$ and H_2O_2. Addition of organic chelating agents which possess abstractable hydrogen atoms was judged to be an inappropriate mode of control on the basis of the reactivity of these reagents with HO·.[15,16,20]

Results and Discussion

Oxidation of $(CN)_5Fe(imz)^{3-}$ by H_2O_2. Figure 1 illustrates the rapid scan spectrum of the reaction between H_2O_2 and $(CN)_5Fe(imz)^{3-}$ at 1.0, 5.0, 20.0, 40.0, and 56.0 s after mixing. No chemical intermediates at substantial concentrations are detectable. A typical oscilloscopic data record of the reaction monitored at 403 nm is shown in Figure 2. An inhibition period is observed early in the reaction. A pseudo-first-order period follows the inhibition. The inhibition period is shortened with increasing [imidazole] at constant pH. The rate is also suppressed with increasing imidazole. The first-order rate constant obtained from the region after inhibition is k_{obsd}. The reciprocal of k_{obsd} is shown in Figure 3 as a function of imidazole at pH 7.0. These data indicate a linear proportionality with $1/k_{obsd}$ tending toward zero in the absence of imidazole. The data which we will present are consistent with the mechanism shown by Scheme I. The rate of formation of $(CN)_5Fe(imz)^{2-}$ is strongly dependent on the competition of HO· for Fe(II) and H_2O_2 in the system. The kinetic scheme may be additionally altered by the presence of radical scavengers if the resultant radical (R·) is reducing for $(CN)_5Fe(imz)^{2-}$. The effect of the organic radical scavengers will be described in a later section.

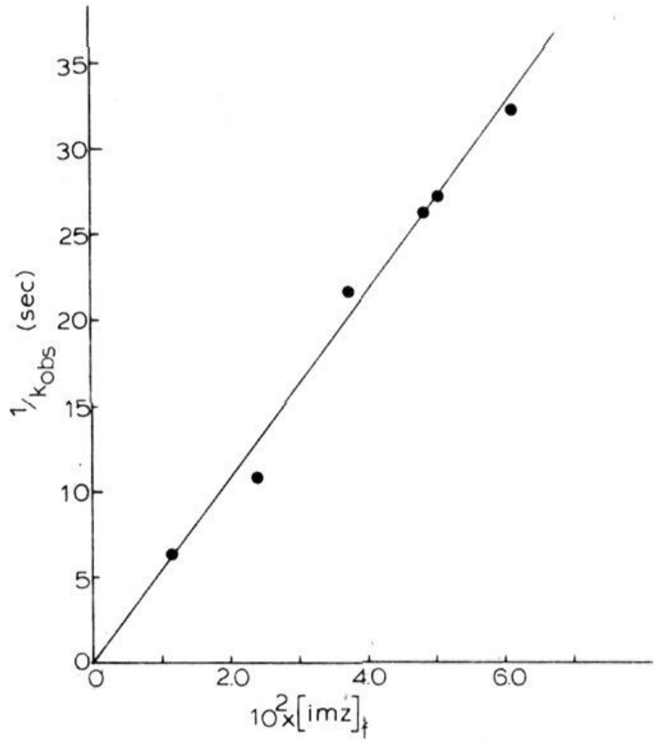

Figure 3. Inhibition of the $(CN)_5Fe\ imz^{3-}/H_2O_2$ reaction by added imidazole: $[(CN)_5Fe(imz)^{3-}] = 2.55 \times 10^{-4}$ M, $[H_2O_2] = 0.103$ M, pH 7.0, $\mu = 0.10$, $T = 25.0$ °C, [imz] = free base ligand concentration calculated with $pK_a = 6.95$, pH measurements, and total analytical concentration of imidazole.

Scheme I

$$(CN)_5Fe(imz)^{3-} \underset{k_{-1}}{\overset{k_1}{\rightleftharpoons}} (CN)_5FeH_2O^{3-} + imz \quad (1)$$

$$K_f = \frac{k_{-1}}{k_1}$$

$$(CN)_5FeH_2O^{3-} + H_2O_2 \xrightarrow{k_2} (CN)_5FeH_2O^{2-} + HO\cdot + OH^- \quad (2)$$

$$(CN)_5FeH_2O^{2-} + (CN)_5Fe(imz)^{3-} \underset{k_{-3}}{\overset{k_3}{\rightleftharpoons}} (CN)_5FeH_2O^{3-} + (CN)_5Fe(imz)^{2-} \quad (3)$$

$$HO\cdot + (CN)_5Fe(imz)^{3-} \xrightarrow{k_4} OH^- + (CN)_5Fe(imz)^{2-} \quad (4)$$

$$HO\cdot + H_2O_2 \xrightarrow{k_5} H_2O + HO_2\cdot \quad (5)$$

$$2HO_2\cdot \xrightarrow{k_6} O_2 + H_2O_2 \quad (6)$$

$$(CN)_5Fe\ imz^{2-} \underset{k_{-7}}{\overset{k_7}{\rightleftharpoons}} (CN)_5FeH_2O^{2-} + imz \quad (7)$$

$$H_3O^+ + imz \overset{1/K_a}{\rightleftharpoons} Himz^+ \quad (8)$$

The kinetic scheme shown by Scheme I predicts a rate law given by eq 9 under the following assumptions: (a) steps 3, 4, 5, 6, and 8 are rapid compared to steps 1, 2, and 7, (b) that the amounts of $(CN)_5FeH_2O^{3-}$ and $(CN)_5FeH_2O^{2-}$ are always very small, (c) that other radicals generated from HO· that are oxidizing for $(CN)_5Fe(imz)^{3-}$ may be represented by the kinetically equivalent step 4,[33] and (d) that the radical reactions between HO· and HO_2· are similar to those studied with

Table I. Rate Constants at 25.0 °C for Scheme I

k_n	Rate	Ref
k_1	$(2.20 \pm 0.21) \times 10^{-3}\ s^{-1}$	This work
k_{-1}	$410 \pm 30\ M^{-1}\ s^{-1}$	This work
k_2	$107 \pm 1\ M^{-1}\ s^{-1}$	17
k_3	$\sim 10^4\ M^{-1}\ s^{-1}$	18, 19
k_4	$\sim 10^{11}\ M^{-1}\ s^{-1}$	20, this work, 21
k_5	$(1.2\text{-}4.5) \times 10^7\ M^{-1}\ s^{-1}$	20
k_6	$7.6 \times 10^5\ M^{-1}\ s^{-1}$	22
k_7	$\leq 2 \times 10^{-4}\ s^{-1}$	This work, 28
k_{-7}	$\sim 50\ M^{-1}\ s^{-1}$	This work, 28

Table II. Hydroxyl Radical Scavenger Effects on $(CN)_5Fe(imz)^{3-}/H_2O_2$ System

HO· Scavenger	k_{HO}, M^{-1} s^{-1} (ref)	HO· mode of reaction	Effect on $(CN)_5$Fe-$(imz)^{3-}/H_2O_2$ system
Imidazole (histidine)	5×10^9 (20)	H abstraction or ring addition	None
tert-Butyl alcohol	4.7×10^8 (20)	H abstraction	None
Acrylonitrile	3×10^9 (23)	Addition	None
H_2EDTA^{2-}	2.8×10^9 (24)	H abstraction	Suppression
H_2O_2	2×10^7 (20)	H abstraction	Suppression

these species and $Fe(CN)_6^{4-/3-}$ by radiolysis methods. The coefficient A may be taken as the fraction of productive events forming $(CN)_5Fe(imz)^{2-}$ from the competition of $(CN)_5Fe(imz)^{3-}$ and H_2O_2 for HO·. If $k_5[H_2O_2] \ll k_4[Fe(II)]av$ $(1 + A) \rightarrow 2.0$; if $k_5[H_2O_2] \simeq k_4[Fe(II)]av$ then $(1 + A) \rightarrow 1.5$; and if $k_5[H_2O_2] \gg k_4[Fe(II)]av$ $(1 + A) \rightarrow 1.0$. [Fe(II)]av is defined as the effective Fe(II) level throughout the run, $[Fe(II)]_0/2$. $[Fe(II)]av = 7.0 \times 10^{-5}$ M in these studies. Some collected rate constants are shown in Table I. The value for k_3 is estimated from the exchange of $Fe(CN)_6^{3-}$ and $(CN)_5Fe(py)^{3-}$ [19] or the $Fe(CN)_6^{4-}/(CN)_5FeH_2O^{2-}$ exchange.[18] These estimates are consistent with the redox potential of $(CN)_5Fe(imz)^{3-/2-}$ within 0.005 V of the $Fe(CN)_6^{4-/3-}$ couple[5] and the rapid oxidation of $(CN)_5Fe(imz)^{3-}$ by $Fe(CN)_6^{3-}$ observed in our laboratory. Steps involving the oxidation of $(CN)_5Fe(imz)^{3-}$ by $HO_2\cdot$ were omitted on the basis of the absence of the oxidation of $Fe(CN)_6^{4-}$ by $HO_2\cdot$.[34] The rate constants in Table I show that assumptions (a) and (b) are met. Assumptions (c) and (d) are in agreement with our observations.

$$\frac{d[(CN)_5Fe(imz)^{2-}]}{dt} = (1 + A) \times \frac{k_2[H_2O_2][(CN)_5Fe(imz)^{3-}]}{K_f[imz]} \qquad (9)$$

$$A = \frac{k_4[Fe(II)]av}{k_4[Fe(II)]av + k_5[H_2O_2]} \qquad (10)$$

$$(1 + A) = \frac{2k_4[Fe(II)]av + k_5[H_2O_2]}{k_4[Fe(II)]av + k_5[H_2O_2]} \qquad (11)$$

$$k_{obsd} = \frac{(1 + A)k_2[H_2O_2]}{K_f[imz]} \qquad (12)$$

The slope of the line defined by the data in Figure 3 is 5.44 × 10^3 M^{-1} s. A rearrangement of eq 12 shows that Scheme I is consistent with the equilibrium induced inhibition of k_{obsd} (eq 13) at constant $[H_2O_2]$. At $[H_2O_2] \simeq 0.10$ M a fractionation factor of 1.8 is observed and the rate appears to be pseudo-first-order in $[H_2O_2]$. Data for the *N*-methylimidazole complex are shown in Figure 4 with a slope of 6.37 × 10^3 M^{-1} s.

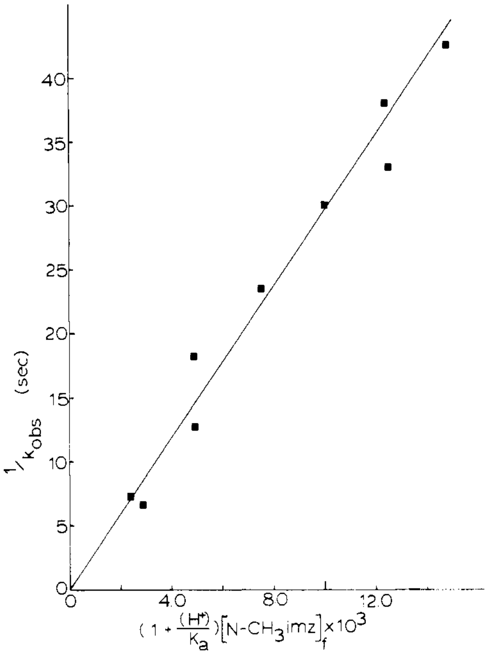

Figure 4. Inhibition of the $(CN)_5Fe(N\text{-}CH_3imz)^{3-}/H_2O_2$ reaction by added *N*-methylimidazole: conditions identical with those of Figure 3, $[N\text{-}CH_3imz]_f$ calculated with $pK_a = 7$.

$$\frac{1}{k_{obsd}} = \frac{K_f}{(1 + A)k_2[H_2O_2]}[imz] \qquad (13)$$

Since the *N*-methylimidazole complex lacks a readily abstractable hydrogen, the reactivities of this complex, $(CN)_5Fe(N\text{-}CH_3imz)^{3-}$, should more nearly satisfy condition (d). Combining $K_f = (1.29 \pm 0.18) \times 10^5\ M^{-1}$ for $(CN)_5Fe(N\text{-}CH_3imz)^{3-}$ with Davies' value of k_2 allows calculation of $(1 + A) = 1.8 \pm 0.2$, which is in very good agreement with $k_4 = 1.10 \times 10^{11}\ M^{-1}\ s^{-1}$, $k_5 = 2 \times 10^7\ M^{-1}\ s^{-1}$. With these values of k_4 and k_5, $(1 + A)$ equals 1.79. Assuming that $(1 + A) = 1.8$ the data from Figure 3 imply that K_f for $(CN)_5Fe(imz)^{3-}$ is $1.05 \times 10^5\ M^{-1}$, which is in reasonable agreement with the kinetically determined value of $(1.86 \pm 0.18) \times 10^5$. The agreement of the kinetic constants using Davies' value for k_2 implies that dissociation of imidazole is followed by substitution controlled reduction of H_2O_2 by $(CN)_5FeH_2O^{3-}$ in the $H_2O_2/(CN)_5Fe(imz)^{3-}$ reaction.

HO· Radical Scavengers. The $(CN)_5Fe(imz)^{3-}/H_2O_2$ system has been studied in the presence of H_2EDTA^{2-}, imidazole, *tert*-butyl alcohol, and acrylonitrile. The effect of addition of these species is shown in Table II. Because two of the necessary components (imidazole and H_2O_2) in the reaction medium are themselves capable of HO· scavenging it is important to consider their effects first. Imidazole inhibition in Figure 3 shows no tendency toward upward curvature in the concentration range of 2.0×10^{-3} to 3.0×10^{-2} M $[imz]_{tot}$. If formation of imidazyl radicals were competitive for H_2O_2 scavenging in a manner that netted a reducing radical for $(CN)_5Fe(imz)^{2-}$ or a dimer diamagnetic product, increasing the imidazole concentration should enhance the suppression of the rate by either of these paths in addition to the equilibrium suppression shown by Scheme I. The absence of any marked upward trend in the data with increasing [imz] implies that if imidazyl radicals are formed, these species are kinetically equivalent to step 4. (Under conditions where [imz]:$[H_2O_2]$:[*tert*-butyl alcohol] were 2×10^{-2}:1:1 no additional inhibition could be detected; when $[H_2O_2]$/[*tert*-butyl alcohol] = 1.0, *tert*-butyl alcohol has a kinetic factor advantage of about

Table III. Effect of H_2EDTA^{2-} on $(CN)_5Fe(imz)^{3-}$ Oxidation[a]

10^2[imz]	$10^2[H_2EDTA]^{2-}$	10^2k_{obsd}, s^{-1}
1.02	0.00	3.68, 3.61
1.02	1.00	2.55
1.03	5.00	2.55
1.03	2.50	2.55
1.03	0.50	2.55
1.01[b]	0.50	2.23[b]

[a] $[H_2O_2] = 0.100$, $\mu = 0.10$ phosphate, $T = 25.0$ °C. [b] *N*-Methylimidazole complex same conditions.

20.) The absence of an experimentally discernible difference in rate allows the inference that the radical of *tert*-butyl alcohol acts only by oxidizing Fe(II).

H_2EDTA^{2-} added to the reaction medium causes a significant retardation in the rate. A sample at high imidazole (~5.8 × 10^{-3} M in free base) which shows almost no inhibition period is strongly inhibited by addition of H_2EDTA^{2-}. The inhibition period is returned upon addition of H_2EDTA^{2-} at the same [imz]. Maximum rate suppression is already achieved at 5.0 × 10^{-3} M H_2EDTA^{2-} as shown in Table III. The value of k_{obsd} at 5.0 × 10^{-3} M H_2EDTA^{2-} is 0.68 ± 0.01 of its value in the absence of H_2EDTA^{2-} for both the $(CN)_5Fe(imz)^{3-}$ and $(CN)Fe(N\text{-}CH_3imz)^{3-}$ oxidations by H_2O_2. Walling has proposed that HO· extracts hydrogen from the ethylenediamine backbone of H_2EDTA^{2-}. The resultant radical is a reducing radical for Fe(III) (eq 14, 15).[24] Maximum suppression of the rate is already achieved by the addition of 5.0 × 10^{-3} M H_2EDTA^{2-}.

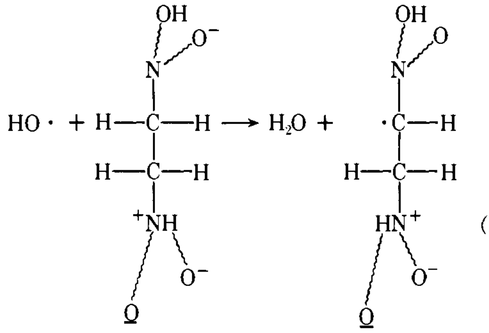

(R·)

(14)

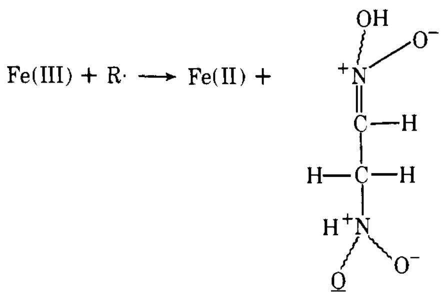

(15)

The good agreement of the slopes defined by Figures 3 and 4 and the relationship of eq 8 shows that the suppression caused by free imidazoles in the reaction medium is due to the reversal of reaction 1 rather than a redox inhibition as found for H_2EDTA^{2-}. If imidazyl radicals were formed and if these radicals were reducing for Fe(III), there would be a positive intercept shown in Figures 3 and 4. The absence of an intercept other than zero is in agreement with the concept that imidazyl radicals are only oxidizing for Fe(II) and therefore kinetically equivalent to HO·. These observations are consistent with Wang's postulates concerning the reactivities of imidazyl species.[6]

Acrylonitrile is also a scavenger for HO· as shown in eq 16. The resultant radical must be rapidly reducible by $(CN)_5Fe(imz)^{3-}$. The rate obtained in the presence of [acrylonitrile] = 6.0 × 10^{-3} M reproduced the rate obtained for the same mixture in the buffer alone within ±1%:$[(CN)_5Fe(imz)^{2-}]_i$ = 4.90 × 10^{-3}, $[imz]_{tot}$ = 1.42 × 10^{-3}, μ = 0.10, T = 25.0 °C, pH phosphate 6.86 (k_{obsd} = 5.78 × 10^{-3} s^{-1}).

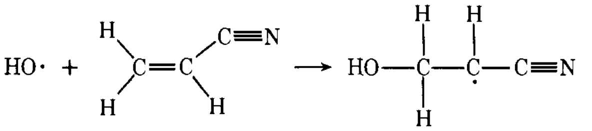

(16)

Hydrogen Ion Dependence. Assignment of step 2 in Scheme I as the rate-limiting step is in agreement with the absence of a hydrogen ion term in eq 8. The oxidation of $Fe(CN)_5H_2O^{3-}$ by H_2O_2 is independent of pH from 5.0 to 9.0.[17] Substitution of HO_2^- is slower than H_2O_2 on $(CN)_5FeH_2O^{3-}$. At higher pH values Davies reports a drop in the rate consistent with

$$k_{obsd} = \frac{2(k_2 + k_2'K_a/[H_3O^+])}{1 + \dfrac{K_a}{[H_3O^+]}}[H_2O_2]_{tot} \qquad (17)$$

where k_2' is the analogous redox process with HO_2^- as step 2 for H_2O_2. K_a for H_2O_2 at 25.0 °C is 2.15 × 10^{-12} M.[25] Our attempts to study the $(CN)_5Fe(imz)^{3-}$ system under conditions where any appreciable amount of HO_2^- is present gave complicated results. At the higher pH values (>9.5) the initial rates are strongly suppressed in agreement with the data of Davies for the lower reactivity of HO_2^-. The experimental difficulties originate in comparable affinities of OH^- and imidazole for the Fe(III) oxidation state in the product (equilibria 18 and 19).

$$(CN)_5Fe(imz)^{2-} + OH^- \rightleftharpoons (CN)_5FeOH^{3-} + imz \qquad (18)$$

$$2(CN)_5FeOH^{3-} \rightleftharpoons 2OH^- + Fe_2(CN)_{10}{}^{4-} \qquad (19)$$

$(CN)_5FeOH^{2-}$, $(CN)_5Fe(imz)^{2-}$, and $Fe_2(CN)_{10}{}^{4-}$ were present in the equilibrium reaction mixture in amounts dependent upon the total free imidazole present, reaction time, and the pH. The initial period of the reaction is obscured by the inhibition period and there are problems presented by the O_2 evolution due to the formation of $(CN)_5FeOH^{3-}$ in the presence of H_2O_2. For these reasons, studies at lower hydrogen ion conditions were not pursued further. No attempt was made to explore the pH range below 6.0 because the competition of H_3O^+ for imidazole compared to $(CN)_5Fe^{3-}$ is favorable in solutions below pH 6.0.[5]

Reaction Stoichiometry. The evolution of O_2 is observed in standing solutions of $(CN)_5Fe(imz)^{2-}$ in the presence of H_2O_2. Table IV illustrates four attempts to define the ratio of H_2O_2:$(CN)_5Fe(imz)^{3-}$. In the presence of a ninefold excess of free ligand, designed to prevent formation of μ-cyano bridged Fe(II) and Fe(III) species, the amount of H_2O_2 consumed was always greater than 0.500 and dependent on the temperature and reaction conditions. Experiments were also conducted in the presence of 0.01 M H_2EDTA^{2-} to scavenge trace metals in buffer salts in order to reduce the rate of H_2O_2 thermal decomposition. The data extrapolated to zero time gave a value of 0.51 ± 0.10 for $[H_2O_2]$ consumed: $[(CN)_5Fe(imz)^{2-}]$ formed. The limiting stoichiometry for oxidation of $(CN)_5Fe(imz)^{3-}$ by H_2O_2 is 2:1. The product, $(CN)_5Fe(imz)^{2-}$, and species at equilibrium with $(CN)_5Fe(imz)^{2-}$ produce a substantial catalase activity of O_2. The catalyzed decomposition of H_2O_2 is responsible for values in Table IV exceeding the 0.500 predicted stoichiometry. The data presented in Figure 5 for the catalytic decomposition of H_2O_2 at pH 6.86 may be given by the rate law

$$\frac{-d[H_2O_2]}{dt} = k_d[H_2O_2]^2[(CN)_5Fe(imz)^{2-}] \qquad (20)$$

Table IV. H_2O_2 Consumed in Reduction of $(CN)_5Fe\ imz^{3-}$

Run	Reaction time	$[(CN)_5Fe\ imz^{2-}] \times 10^2$	% Fe total as $(CN)_5Fe\ imz^{2-}$	$10^2[H_2O_2]$ consumed	$\frac{[H_2O_2]\ \text{cons at}\ t}{[(CN)_5Fe\ imz^{2-}]_t}$
1A[a]	5 min	1.13	72.9	0.61	0.54
1B	15 min	1.28	82.6	0.91	0.71
1C	30 min	1.37	88.4	1.19	0.87
1D	45 min	1.39	89.7	1.24	0.89
1E	1.0 h	1.43	92.2	1.53	1.07
1F	1.5 h	1.45	93.5	1.67	1.15
1G	2.0 h	1.49	96.1	1.81	1.22
2A[b]	1.0 h	1.38	89.0	1.43	1.04
2B	3.0 h	1.52	98.1	1.65	1.09
2E	5.0 h	1.55	100.0	1.70	1.10
3A[c]	5.0 h	1.81	90.7	1.24	0.68
3B	8.5 h	1.91	95.5	1.92	1.00
4A[d]	3.0 h	1.72	86.5	1.80	1.05
4B	6.0 h	1.81	91.0	2.25	1.24
		a	b	c	d
$[Fe(CN)_5imz^{3-}]_i$		1.55×10^{-2} M	1.55×10^{-2} M	2.00×10^{-2} M	1.99×10^{-2} M
$[H_2O_2]_i$		4.12×10^{-2}	3.90×10^{-2}	4.20×10^{-2}	4.27×10^{-2}
$[imz]_{tot}$		1.53×10^{-2}	1.56×10^{-2}	0.184	0.184
Temp, °C		24	24	18	22

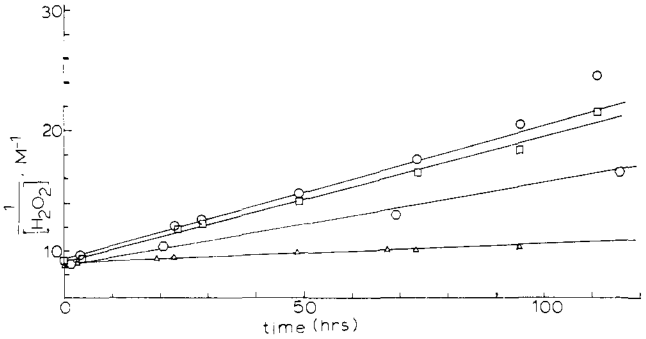

Figure 5. Catalase activity of $(CN)_5Fe(imz)^{2-}$: ⊙, $[(CN)_5Fe(imz)^{2-}]$ = [III] = 4.86×10^{-3} M; ⊡, [III] = 4.86×10^{-3} M; ○, [III] = 2.38×10^{-3} M, [*tert*-butyl alcohol] = 1.14×10^{-2} M; △, [III] = 0; in each $[H_2O_2]_0$ = 0.114 M, [EDTA] = 0.01 M, μ = 0.075 phosphate/EDTA, T = 25.0 °C, protected from light.

Catalase activity experiments were conducted in the dark at 25.0 °C, $\mu = 0.10$, in phosphate buffer. Analysis for H_2O_2 was carried out by titration with Ce(IV) after separation of H_2O_2 by anion exchange as described in the Experimental Section. Figure 5 shows the second-order behavior for the decomposition of H_2O_2 at two different concentrations of $(CN)_5Fe(imz)^{2-}$ and in the presence and absence of *tert*-butyl alcohol. Walling has shown that the catalytic decomposition of H_2O_2 by $Fe(H_2O)_6{}^{3+}$ proceeds via a radical chain pathway which is suppressed by HO· scavengers such as acetone and *tert*-butyl alcohol.[24] The specific third-order decomposition of H_2O_2 rate, k_d, is $8.4 \times 10^{-8}\ M^{-2}\ s^{-1}$ in the absence of *tert*-butyl alcohol. Measurements of the H_2O_2 decomposition rate are corrected for all decomposition pathways determined for the blank. With *tert*-butyl alcohol added at a level of $[H_2O_2]_0/[\textit{tert}\text{-butyl alcohol}]_0 = 10$, a 7.6% decrease is observed in k_d. The small magnitude of the effect exerted by *tert*-butyl alcohol is consistent with competitive scavenging of HO· by H_2EDTA^{2-} and *tert*-butyl alcohol. A similar effect of H_2EDTA^{2-} and *tert*-butyl alcohol is observed in the catalase activity of $Fe(EDTA)^-$.[24] A rate law for the catalytic decomposition of H_2O_2 by an Fe(III) complex is generally other than a $[H_2O_2]^2$ dependence unless the hydroxyl radical chain is *strongly* retarded by HO· radical scavengers.[15,16]

Effect of Added $(CN)_5Fe(imz)^{2-}$. An attempt was made to determine the effect of the Fe(III) product on the rate shown by the curves in Figure 6. The maximum enhancement is a function both of added $(CN)_5Fe(imz)^{2-}$ and the amount of free imidazole in the reaction medium (Table V). Increasing $[Fe(III)]_0$ by a factor of nearly 10 at constant imidazole shows a rate increase in runs B and D of about 30%. However, in experiments C and D at twice the concentration of $[Fe(III)]_0$ and a 1.26 increase in imidazole shows a decrease of 20% in rate of the $(CN)_5Fe(imz)^{3-}$ oxidation by H_2O_2. The results are in qualitative agreement with Scheme I. Increasing the concentration of $(CN)_5Fe(imz)^{2-}$ increases the available pool of $(CN)_5FeH_2O^{2-}$. The cycle shown by Scheme II provides an alternate source of HO_2· and HO· which may contribute to the oxidation of $(CN)_5Fe(imz)^{3-}$. The effect of the suppression caused by imidazole via equilibria 1 and 7 in Scheme I is evident for runs C and D. In the absence of added $(CN)_5Fe(imz)^{2-}$ increasing free imidazole 1.38-fold suppresses the rate by 10% (runs E and A). It should be noted that all of the data presented in Figure 6 and Table V were obtained in the presence of H_2EDTA^{2-}. H_2EDTA^{2-} was added to assure chelation of any $Fe(H_2O)_6{}^{3+}$ which might be generated from thermal decomposition of the iron complexes.[26] A sequence similar to Scheme II has been given by Barb, Baxendal, George, and Hargrave[32] for the ferric ion catalyzed decomposition of H_2O_2.

Scheme II

$$(CN)_5FeH_2O^{2-} + H_2O_2 \rightarrow (CN)_5FeH_2O^{3-} + HO_2\cdot + H_3O^+ \qquad (21)$$

$$(CN)_5FeH_2O^{3-} + H_2O_2 \rightarrow (CN)_5FeH_2O^{2-} + HO\cdot + OH^- \qquad (22)$$

$$HO_2\cdot + (CN)_5FeH_2O^{2-} \rightarrow H_3O^+ + (CN)_5FeH_2O^{3-} + O_2 \qquad (23)$$

$$HO_2\cdot + (CN)_5Fe(imz)^{3-} \rightarrow (CN)_5Fe(imz)^{3-} + O_2 + H^+ \qquad (24)$$

$$HO\cdot + (CN)_5Fe(imz)^{3-} \rightarrow (CN)_5Fe(imz)^{2-} + HO^- \qquad (25)$$

H_2O_2 Dependence. Equations 11 and 12 predict a nonlinear dependence on $[H_2O_2]$; at low $[H_2O_2]$ where $(1 + A)$ approximates 2.0 a linear dependence in $[H_2O_2]$ is anticipated. This effect is observed for all of the data in Figure 6 at the lower concentrations (≤0.03 M). At $[H_2O_2] > 0.10$ M a slight suppression is observed. At the high H_2O_2 limit eq 12 predicts a linear dependence in $[H_2O_2]$ at one-half the slope of the low

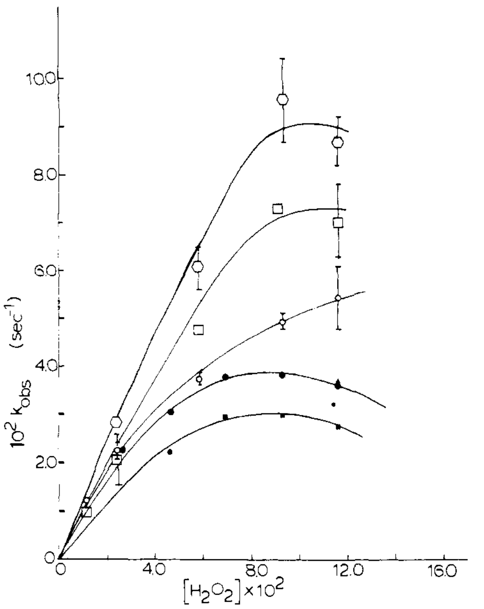

Figure 6. Effect of added $(CN)_5Fe(imz)^{2-}$ and imidazole on the $(CN)_5Fe(imz)^{3-}/H_2O_2$ reaction: conditions as described in Table V, run A ■, run B ○, run C ○, run D □, run E ●; solid lines are for illustrative purposes only.

Table V. Effect of Added $(CN)_5Fe(imz)^{2-}$ and Imidazole on the Oxidation of $(CN)_5Fe(imz)^{3-}$[a]

$10^4[Fe(III)]_0$	$[Fe(III)]_0/[Fe(II)]_0$	$10^3[imz]_{free}$	10^2k_{limit}	Run
0.000	0.00	1.17	3.0	A
1.223	0.863	4.98	5.5	B
6.05	4.66	4.00	9.0	C
12.10	9.33	5.02	7.2	D
0.00	0.00	0.86	4.4	E

[a] 25.0 °C, μ = 0.10 phosphate, $[H_2EDTA^{2-}]$ = 0.01 M, $[Fe(CN)_5imz^{3-}]_0 = 1.30 \times 10^{-4}$ M, pH 6.86.

Table VI. Temperature Dependence of Imidazole Dissociation[c]

Ligand	Temp, °C	$10^3/T$, K^{-1}	10^3k, s^{-1}	$-\mathrm{Ln}(k/T)$
imz[a]	25.0	3.354	2.03	11.90
	30.0	3.299	3.45	11.38
	32.8	3.268	4.90	11.05
	35.0	3.245	6.23	10.81
	40.0	3.193	11.1	10.25
N-CH_3imz[b]	25.0	3.354	3.24	11.43
	30.0	3.299	5.85	10.86
	35.0	3.245	9.48	10.39
	40.0	3.193	16.3	9.86

[a] Average of three experiments. [b] Average of two experiments. [c] $[2CH_3pz]$ = 0.100 M, $[(CN)_5Fe(imz\text{-}R)^{3-}]_0 = 1.40 \times 10^{-4}$ M, μ = 0.10 (phosphate), pH 6.86, $[imz\text{-}R]_{tot} = 1.0 \times 10^{-2}$ M.

Table VII. Activation Parameters for Imidazole Dissociation

Ligand	10^3k_{298}, s^{-1}	$\Delta H^{\ddagger}$, kcal/mol	$\Delta S^{\ddagger}$, cal/mol K
Imidazole	2.20 ± 0.21	21.5 ± 0.5	+1 ± 2
1-Methylimidazole	3.24 ± 0.22	19.1 ± 0.5	−5 ± 2

limit domain. The effect of the slight suppression may be interpreted as all HO· species being scavenged by H_2O_2 (eq 5). The level of $HO_2\cdot$ produced is then sufficient to produce a slight inhibition by steps 23, 24, and 3. Since the reduction of Fe(III) species by $HO_2\cdot$ was not considered in the derivation of eq 12, it is no longer valid above $[H_2O_2]$ = 0.10 M where $[H_2O_2]_0/[(CN)_5Fe(imz)^{3-}]_0 \gtrsim 10^3$. Under these conditions assuming an estimate of 1.1×10^4 M^{-1} s^{-1} for k_4, virtually all HO· is scavenged by H_2O_2 forming $HO_2\cdot$. Steps equivalent to (23) and (24) will increasingly retard the rate of production of $(CN)_5Fe(imz)^{2-}$ as larger fraction of inhibitory events occur at high $[H_2O_2]$.

Dissociation of $(CN)_5Fe(imz)^{3-}$ and $(CN)_5Fe(N\text{-}CH_3imz)^{3-}$. The value of k_1 was measured at pH 6.86, μ = 0.10 (phosphate), under Ar in thermostated cells. The dissociation step was monitored by scavenging of the $(CN)_5FeH_2O^{3-}$ by a large excess of 2-methylpyrazine. Absorbance-time data were taken at 450 nm, the maxima of $(CN)_5Fe(2CH_3pz)^{3-}$. The rate was found to be independent of the scavenging ligand at $[2CH_3pz]$ = 0.0100, 0.0251, 0.0501, and 0.100 M. The reaction is dissociative and follows the sequence in Scheme III.

Scheme III

$$(CN)_5Fe(imz)^{3-} + H_2O \underset{k_{-1}}{\overset{k_1}{\rightleftharpoons}} (CN)_5FeH_2O^{3-} + imz \tag{26}$$

$$(CN)_5FeH_2O^{3-} + 2CH_3pz \underset{k_{-27}}{\overset{k_{27}}{\rightleftharpoons}} (CN)_5Fe(2CH_3pz)^{3-} + H_2O \tag{27}$$

Using the steady-state approximation, the rate for ligand exchange is given by

$$\frac{-d[(CN)_5Fe(imz)^{3-}]}{dt[(CN)_5Fe(imz)^{3-}]} = \frac{k_1k_{27}[pz] + k_{-1}k_{-27}[imz]}{k_{-1}[imz] + k_{27}[pz]} \tag{28}$$

Under conditions where $k_1k_{27}[pz] \gg k_{-1}k_{-27}[imz]$ and $k_{-1}[imz] \ll k_{27}[pz]$, $k_{obsd} = k_1$. The systems were studied where $[imz] \ll [pz]$ and the reverse constants are 10^5 less than the forward constants. The value of k_1 equals (2.20 ± 0.21) $\times 10^{-3}$ s^{-1} at 25.0 °C. The temperature-dependent data are presented in Table VI for the $(CN)_5Fe(imz)^{3-}$ and the analogous 1-methylimidazole complex. Activation parameters obtained from the Eyring rate theory are summarized in Table VII. The 1-methylimidazole complex exhibits a lower $\Delta H^{\ddagger}$ by 2.4 kcal/mol and a more negative $\Delta S^{\ddagger}$ by 6 units (Table VII). We propose that the difference in the activation parameters originates in a cage effect of solvent water for $(CN)_5Fe(imz)^{3-}$ and $(CN)_5Fe(N\text{-}CH_3imz)^{3-}$. Imidazole is more stable in solution than 1-methylimidazole because the hydrogen atom on the pyrrole nitrogen can hydrogen bond to surrounding "cage" water molecules. The methyl group of N-methylimidazole cannot. The established polarity of the NH of the pyrrole moiety makes imidazole a slightly better π acceptor. The dissociation of imidazole costs more in $\Delta H^{\ddagger}$ to overcome the π interaction. The same factors control the more negative $\Delta S^{\ddagger}$ observed for removal of 1-methylimidazole from its $(CN)_5Fe^{3-}$ complex. Imidazole is less disruptive of solvent structure in transferring from the caged, more solvated, complex into the bulk solvent. The 1-methylimidazole costs more in solvent reordering in its dissociation which is observed as a more negative $\Delta S^{\ddagger}$.

Formation of $(CN)_5Fe(N\text{-}CH_3imz)^{3-}$. The formation of the 1-methylimidazole complex was studied by the competition technique with 2-methylpyrazine as the indicator ligand at constant concentration. The observed rate constant for the formation of the kinetically distributed mixture of $(CN)_5Fe(2CH_3pz)^{3-}$ and $(CN)_5Fe(N\text{-}CH_3imz)^{3-}$ products obeys

$$k_{obsd} = k_{2CH_3pz}[2CH_3pz] + k_{N\text{-}CH_3imz}[N\text{-}CH_3imz] \tag{29}$$

The value of k_{2CH_3pz} was determined on independent stopped-flow experiments in the absence of N-CH_3imz as 332

± 6 M^{-1} s^{-1}. Data obtained for the competition experiments showed a linear response in [N-CH_3imz] with the intercept at 3.32 s^{-1} for a constant 0.0100 M 2CH_3pz level. The slope obtained from the competition study yields $k_{N\text{-}CH_3imz}$ = 418 ± 20 M^{-1} s^{-1}. The association constant for $(CN)_5Fe(N\text{-}CH_3imz)^{3-}$ is then calculated to be 1.29 ± 0.18 × 10^5 M^{-1} from the kinetic constants at 25.0 °C. No term in the rate law corresponding to the reactivity of the protonated form of *N*-methylimidazole was observed. However, the protonated form of imidazole is reactive toward $(NH_3)_5RuOH_2^{2+}$ [29]

Formation of $(CN)_5Fe(imz)^{3-}$. Equivalent competition experiments between imidazole and 2-methylpyrazine were conducted. The rate measured as the free-base imidazole concentration tended to zero was in agreement with the intercept term, k_{2CH_3pz}[pz], as in eq 29. From the observations of the 1-methylimidazole data and the imidazole results it is seen that little preferential association of $(CN)_5FeH_2O^{3-}$ for $imzH^+$ or imz relative to the neutral 2CH_3pz moiety occurs. From the slope of the line defined by the analogous equation as in (29), k_{imz} was evaluated as 410 ± 30 M^{-1} s^{-1}. Therefore k_{imz} and $k_{N\text{-}CH_3imz}$ are virtually equal. The value of k_{imz} (410 M^{-1} s^{-1}) is in fair agreement with 231 M^{-1} s^{-1} calculated by means of the value of K_f determined from the redox experiments (1.05 × 10^5 M^{-1}) and the dissociation rate constant 2.20 × 10^{-3} s^{-1}. The values of K_f determined by the redox method is important because the complexation mechanism of $(CN)_5FeH_2O^{3-}$ by imidazole is complicated by the dimerization of $(CN)_5FeH_2O^{3-}$ into $Fe_2(CN)_{10}^{6-}$. The second-order rate constants for complexation by imz and N-CH_3imz are in excellent agreement with Malin's values for the substituted pyridines and pyrazines.[31] By contrast, the dissociation behavior of $Himz^+$ from $(CN)_5Fe(imz)^{2-}$ is general acid catalyzed.[28] The observed reactivity is apparently related to the equivalent electronic environment of Fe(II) and Fe(III) in the cyanide complexes.[27,28]

The high association constants of imidazole for the Fe(II) complex (1.86 × 10^5 M^{-1}) and the Fe(III) oxidation state (3.6 × 10^5 M^{-1})[28] (cf. Table I) assure that the pool of $(CN)_5FeH_2O^{3-}$ and $(CN)_5FeH_2O^{2-}$ is always small. The reactivities of HO· and HO_2· are consistent with the pulse radiolysis studies of these species for $Fe(CN)_6^{3-}$ and $Fe(CN)_6^{4-}$. The HO· is certainly involved in the mechanism of the oxidation of the imidazole complexes on the basis of (1) the suppression of the rate as a function of H_2O_2 and H_2EDTA^{2-} and the competition of kinetic events of HO· for $(CN)_5Fe(imz)^{3-}$ and H_2O_2 at low [H_2O_2], (2) the equivalence of the observed rate expression to the known reactivity of H_2O_2 with $(CN)_5Fe(H_2O)^{3-}$, (3) the absence of any evidence of imidazyl-Fe(III) complexes as kinetic intermediates, and (4) the similarity in effect of various organic radical scavengers for HO· and their corresponding reactivity with Fe(II) and Fe(III) in the media.

We have pulse radiolysis experiments in progress to determine the actual value of the kinetic constants for HO· and HO_2· with $(CN)_5Fe(imz)^{3-}$ and related complexes.[30]

Acknowledgment. We gratefully acknowledge the assistance of the Research Corporation for funds that enabled us to purchase the stopped-flow spectrophotometer and to support these studies.

References and Notes

(1) E. Antonini and M. Brunori, "Hemoglobin and Myoglobin in Their Reactions with Ligands", North-Holland Publishing Co., Amsterdam, 1971.
(2) D. A. Baldwin, R. M. Pfeiffer, D. W. Reichgott, and N. Rose, *J. Am. Chem. Soc.*, **95**, 4087 (1973).
(3) D. V. Stynes, H. C. Stynes, B. R. James, and J. A. Ibers, *J. Am. Chem. Soc.*, **95**, 4087 (1973).
(4) G. N. La Mar and F. A. Walker, *J. Am. Chem. Soc.*, **95**, 1782 (1973); G. N. La Mar, J. D. Satterlee, and R. V. Snyder, *ibid.*, **96**, 7137 (1974); F. A. Walker, M. Lo, and M. T. Ree, *ibid.*, **98**, 5552 (1976).
(5) R. E. Shepherd, *J. Am. Chem. Soc.*, **98**, 3329 (1976).
(6) J. H. Wang, *Acc. Chem. Res.*, **3**, 90 (1970), and references cited therein.
(7) L. E. Bennett, *Prog. Inorg. Chem.*, **18**, 1 (1973), and references cited therein.
(8) (a) B. Lal, *Curr. Sci*, **16**, 118 (1947); (b) J. H. Baxendale, *Adv. Catal.*, **4**, 31 (1952); (c) J. Sobokowski, *Rocz. Chem.*, **43**, 1729 (1969).
(9) C. Walling, *Acc. Chem. Res.*, **8**, 125 (1975).
(10) (a) G. Emschwiller and J. Legros, *C. R. Acad. Sci.*, **261**, 1535 (1965); (b) G. Emschwiller, *ibid.*, **268**, 695 (1969).
(11) G. Davies and A. R. Garafolo, *Inorg. Chim. Acta*, **19**, L3 (1976).
(12) We thank Professors D. W. Margerum and H. L. Pardue of the Department of Chemistry, Purdue University, for use of their Vidicon spectrophotometer and automated stopped-flow for a number of early experiments on this research.
(13) B. Jaselskis, *J. Am. Chem. Soc.*, **83**, 1082 (1961).
(14) J. H. Espenson and S. G. Wolenuck, *Inorg. Chem.*, **11**, 2034 (1972).
(15) C. Walling and A. Goosen, *J. Am. Chem. Soc.*, **95**, 2987 (1973).
(16) C. Walling and G. El-Taliawi, *J. Am. Chem. Soc.*, **95**, 844 (1973).
(17) G. Davies and A. R. Garafolo, *Inorg. Chem.*, **15**, 1101 (1976).
(18) R. Stasiw and R. G. Wilkins, *Inorg. Chem.*, **8**, 156 (1969).
(19) H. E. Tomá and J. M. Malin, *J. Am. Chem. Soc.*, **97**, 288 (1975).
(20) L. M. Dorfman and G. E. Adams, "Reactivity of the Hydroxyl Radical in Aqueous Solutions", NSRDA—NBS 46 publication, 1973.
(21) J. Rabini and M. S. Matheson, *J. Am. Chem. Soc.*, **86**, 3175 (1964), with estimates based on ref 19.
(22) J. Rabini and M. S. Matheson, *J. Phys. Chem.*, **70**, 761 (1966).
(23) Estimate based on acrylamide, ref 20.
(24) C. Walling, R. E. Partch, and T. Weil, *Proc. Natl. Acad. Sci. U.S.A.*, **72**, 140 (1975).
(25) M. G. Evans and N. Uri, *Trans. Faraday Soc.*, **45**, 225 (1949).
(26) H. E. Toma, *Inorg. Chim. Acta*, **15**, 205 (1975).
(27) A. Calabrese and R. G. Hayes, *J. Am. Chem. Soc.*, **96**, 5051 (1974).
(28) W. J. Dressick and R. E. Shepherd, work in progress for the NCS^- substitution on $(CN)_5Fe(imz)^{2-}$
(29) R. E. Shepherd and H. Taube, *Inorg. Chem.*, **12**, 1392 (1973).
(30) In collaboration with M. Z. Hoffman of the Department of Chemistry, Boston University.
(31) H. E. Toma and J. M. Malin, *Inorg. Chem.*, **12**, 2080 (1973); ref 17.
(32) W. G. Barb, J. H. Baxendale, P. George, and K. R. Hargrave, *Trans. Faraday Soc.*, **47**, 591 (1951).
(33) A referee has observed that although HO· will have a distinct rate ratio in its reactions with Fe(II) and H_2O_2, the radicals R· formed from RH and HO· will almost necessarily have a different kinetic ratio for the same two reductants. R· can never be perfectly kinetically equivalent to HO· in the limit that Fe(II) reduces R· by a factor of ≈ 10^3 faster than H_2O_2 (cf. Table I) a fractionation factor *A* will be maintained that is not discernible as different from the HO· fractionation factor within experimental error.
(34) G. Hughes and C. Willis, *J. Chem. Soc.*, 4848 (1962).